# Magnetic interaction between copper (II) ion and paramagnetic NO and O 2 molecules in Y-type zeolite at low temperature: An EPR study

**ARTICLE** *in* MICROPOROUS AND MESOPOROUS MATERIALS · SEPTEMBER 2005

Impact Factor: 3.45 · DOI: 10.1016/j.micromeso.2005.04.011



**3 AUTHORS**, INCLUDING:

Hidenori Yahiro
Ehime University
**112** PUBLICATIONS **3,692** CITATIONS
SEE PROFILE

Masaru Shiotani
Hiroshima University
**204** PUBLICATIONS **2,470** CITATIONS
SEE PROFILE

Available online at www.sciencedirect.com
SCIENCE DIRECT®
Microporous and Mesoporous Materials 83 (2005) 165–171
MICROPOROUS AND MESOPOROUS MATERIALS
www.elsevier.com/locate/micromeso

# Magnetic interaction between copper (II) ion and paramagnetic NO and $O_2$ molecules in Y-type zeolite at low temperature: An EPR study

Hidenori Yahiro [a,b,*], Yasuo Ohmori [a], Masaru Shiotani [a]

[a] Department of Applied Chemistry, Faculty of Engineering, Hiroshima University, Higashi-Hiroshima 739-8527, Japan
[b] Department of Applied Chemistry, Faculty of Engineering, Ehime University, Matsuyama 790-8577, Japan

Received 30 November 2004; received in revised form 18 April 2005; accepted 19 April 2005
Available online 4 June 2005

**Abstract**

Electron paramagnetic resonance (EPR) spectra of partially copper ion exchanged Na-Y zeolite (CuNa-FAU) were measured in the presence of paramagnetic gases such as nitrogen monoxide (NO) and oxygen ($O_2$) as a function of temperature (110–270 K). The EPR signal intensities of the $Cu^{2+}$ ions deviated from those predicted by Curie's paramagnetic law due to the magnetic interaction between the $Cu^{2+}$ ions and paramagnetic gaseous molecules adsorbed on the zeolites; the minimum signal intensity was observed at 150–170 K for CuNa-FAU with NO and the maximum intensity was observed at 170–190 K for CuNa-FAU with $O_2$. The temperature dependent signal intensities, accompanying the NO adsorption, were discussed in terms of the Langmuir adsorption model in the higher temperature range of 150–190 K.


*Keywords:* Copper ion; Nitrogen monoxide; Oxygen; Electron paramagnetic resonance; Magnetic interaction; Y-type zeolite

## 1. Introduction

Zeolites containing transition metal ions have been widely studied because of their interesting adsorptive and catalytic properties. It has been well established that, in zeolite matrices, the transition metal ions are highly dispersed and can occupy specific coordination sites after dehydration [1,2]. Parts of them can act as an adsorptive or a catalytically active site in general. A large number of studies, concerning the valence and the distribution of transition metal ions exchanged into zeolites, the coordination number of metal ion with the oxygen atoms in zeolite framework, and the adsorption of reactants on metal ions, have been reported by using various spectroscopic methods [1–9].

Among spectroscopies, electron paramagnetic resonance (EPR) is the most powerful method to characterize the paramagnetic transition metal ions in zeolites, especially for $Cu^{2+}$ ions isolated in zeolites because of its high sensitivity. One of the recent demands of EPR and its related techniques for studying copper-zeolites is to elucidate the geometric structure of molecule-coordinated $Cu^{2+}$ ions related to the mechanism of the catalytic process. Vigorous studies in this direction have been carried out by Kevan and co-workers [10–13]. They demonstrated by electron spin echo envelope modulation (ESEEM) spectroscopy that $Cu^{2+}$ ions are located in the hydrated copper ion-exchanged ZSM-5 zeolite (Cu-MFI) as paramagnetic $Cu^{2+}$–$OH^-$ with five coordinated water molecules. The geometric structure of the water-coordinated $Cu^{2+}$ ions in ZSM-5 zeolites

* Corresponding author. Address: Department of Applied Chemistry, Faculty of Engineering, Ehime University, Matsuyama 790-8577, Japan. Tel.: +81 89 927 9929; fax: +81 89 927 9946.
*E-mail address:* hyahiro@eng.ehime-u.ac.jp (H. Yahiro).

1387-1811/$ - see front matter © 2005 Elsevier Inc. All rights reserved.
doi:10.1016/j.micromeso.2005.04.011

was proposed by our recent electron nuclear double resonance (ENDOR) study [14]. These studies of the water-coordinated $Cu^{2+}$ ion are important as they give information about the precursor of the catalytically active sites. The coordination of ammonia to $Cu^{2+}$ ions is also of interest, and EPR [15] and ENDOR [14] studies of copper-zeolite with ammonia have successfully provided the geometrical information of $Cu^{2+}$–ammonia complexes.

The nitrogen monooxide (NO) molecule is paramagnetic by itself, and its adsorption state on diamagnetic copper ion, $Cu^{+}$, exchanged into zeolites has been studied by EPR [16,17]. The EPR spectrum of the ($Cu^{+}$–NO) complex formed in Y-type zeolites was first reported by Naccache and Ben Taarit [16]. Sojka et al. [17] reported that the ($Cu^{+}$–NO) complex could be better presented by a chemical species of $Cu^{2+}$–$NO^{-}$ with an end-on bent structure and considered to be an intermediate of the NO decomposition over Cu-MFI catalysts. When paramagnetic NO molecules are introduced into the copper-zeolites having $Cu^{2+}$ ions, it is expected that the magnetic interaction between the paramagnetic $Cu^{2+}$ ion and NO molecule adsorbed on zeolite occurs. The aim of this study is to obtain experimental information about the magnetic interaction by monitoring the progressive changes in the EPR spectral features and the intensity of the paramagnetic $Cu^{2+}$ ion exchanged in Y-type zeolites upon exposure to paramagnetic NO molecules as a function of the measurement temperature (110–270 K). Furthermore, the adsorption behavior of NO on CuNa-Y was compared with that of $O_2$ in the low temperature region.

## 2. Experimental

The sodium-ion-exchanged Y-type zeolite (Na-FAU) with a Si/Al ratio of 5.6 was supplied by Tosoh. Co. Partially copper-ion-exchanged Y-type zeolite (CuNa-FAU) was prepared by the conventional ion-exchange method with copper acetate solution [18]. After filtering, washing with deionized water, and drying overnight at 337 K, the sample was heated at 773 K for 2 h in air. The Cu/Al atomic ratio of the prepared CuNa-FAU determined by the induced coupling plasma (ICP) method was 0.035.

A 0.05 g CuNa-FAU sample was placed into a quartz tube (5 mm in diameter and 200 mm in length). The sample was evacuated at 473 K for 1 h and then heated under pressure less than 1.33 Pa at 773 K for 2 h. After the sample was cooled down to room temperature, 1.0–$3.0 \times 10^{-4}$ mol of $O_2$ or NO was introduced into the sample tube at the same temperature. The X-band EPR spectra were recorded with a Jeol JES-RE1X EPR spectrometer in the temperature range of 110–270 K. The relative number of radicals (or EPR spectral intensity) was evaluated by the double integration of the first derivative EPR spectrum. $Mn^{2+}$/MgO was used as the external reference sample to determine both the *g*-values and EPR spectral intensities of $Cu^{2+}$.

The magnetic susceptibility of CuNa-FAU with and without the paramagnetic molecules, $O_2$ and NO, was measured using a superconducting quantum interference device (SQUID; Quantum Design MPMS-5S) in the temperature range between 110 and 270 K.

## 3. Results and discussion

### 3.1. EPR spectra of CuNa-FAU

Fig. 1 shows the EPR spectra of the dehydrated CuNa-FAU without any paramagnetic gases. The EPR spectra were recorded at stepwise increasing temperatures from 110 to 270 K. In the spectra, two sets of resolved signals due to the isolated $Cu^{2+}$ ions, marked

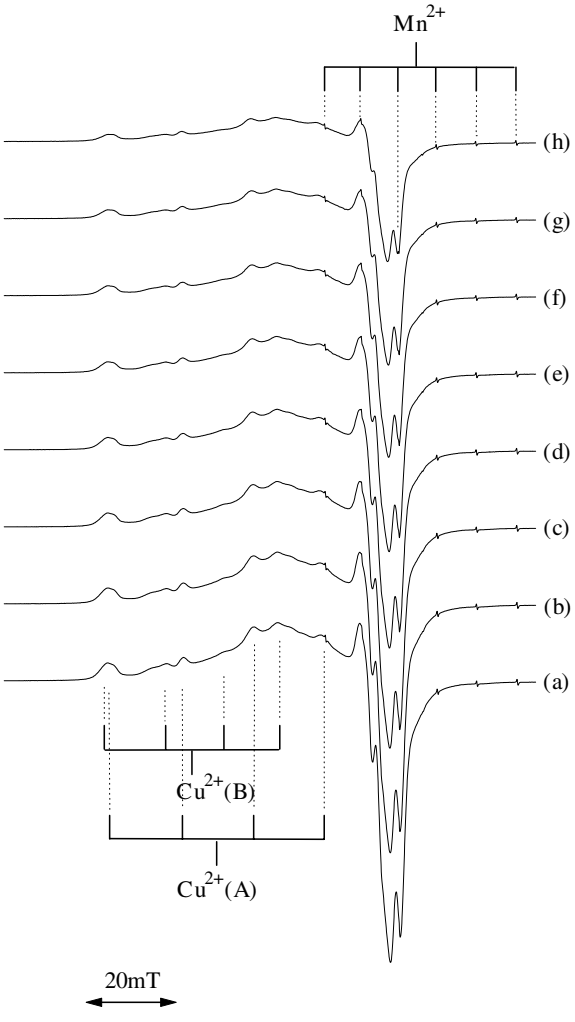


Fig. 1. EPR spectra of "pure" CuNa-FAU (without any paramagnetic gases), recorded at (a) 110, (b) 130, (c) 150, (d) 170, (e) 190, (f) 210, (g) 230, and (h) 270 K. The EPR parameters are given in the text.

as $Cu^{2+}$ (A) and $Cu^{2+}$ (B), were clearly observed as indicated by the sticks. The signals were overlapped by an underlying weak and broad spectrum, which is attributable to the spin-exchange interacting $Cu^{2+}$ ion clusters [19]. The $Cu^{2+}$ (A) signals consist of the parallel component of $g_{//} = 2.32$ and $A_{//} = 15.9$ mT, whereas the $Cu^{2+}$ (B) signals consist of $g_{//} = 2.37$ and $A_{//} = 12.4$ mT. The two sets of EPR parameters deduced from the spectrum are in close correspondence with the previously reported ones [3,20,21]. Pierloot et al. [21] have reported that the different aluminum distributions in the six-ring site give rise to two different sets of *g*-factors, consistent with the presence of two different signals in the EPR spectra of CuNa-FAU and that the signals at $g_{//} = 2.32$ and $g_{//} = 2.37$ were tentatively assigned to $Cu^{2+}$ ion on the six-ring site with one or two Al and to $Cu^{2+}$ on the six-ring site with more than two Al, respectively.

With increasing temperatures from 110 K to 270 K, the line shape remained essentially unchanged, but the EPR intensity gradually decreased. Fig. 2 shows the EPR signal intensity for CuNa-FAU (●) as a function of the reciprocal temperature ($T^{-1}$). For this "pure" CuNa-FAU (i.e., without any introduced paramagnetic molecules), a linear relationship was obtained between the observed relative signal intensity and $T^{-1}$, indicating that the EPR signal intensity obeys Curie's paramagnetic law (represented by the dotted line in Fig. 2). This result means that the number of the $Cu^{2+}$ ions detected by EPR remained constant in the temperature range of 110–270 K.

### 3.2. EPR spectra of CuNa-FAU in the presence of NO

When NO molecules ($^2\Pi_{1/2}$ electronic ground state) are adsorbed on a solid surface, the orbital angular momentum is quenched by the electric fields at the adsorption site, resulting in annulment of the degeneracy between the two antibonding orbitals, $\pi_x^*$ and $\pi_y^*$ and the paramagnetic ground state accessible to EPR measurement is formed [22]. EPR signals assigned to the NO radical adsorbed on a diamagnetic cation such as sodium ion [23–26], proton [25], and lithium ion [27] exchanged into zeolites have been recorded at low temperatures less than 77 K. In the present study, however, no signals assigned to the NO radical were observed for CuNa-FAU, regardless of the amount of NO introduced ($1.0–3.0 \times 10^{-4}$ mol). The failure in the EPR observation of the NO radical can be explained as follows. The NO molecule easily forms a diamagnetic dimer, $(NO)_2$, on solid surfaces at low temperatures; the dimer formation rate increases with decreasing temperatures [28]. The NO molecule escaped from the dimer formation is paramagnetic, but not detectable by EPR in general because of linewidth broadening due to an incomplete lift of the degenerated molecular orbitals and/or rapid molecular location in the zeolite, especially,

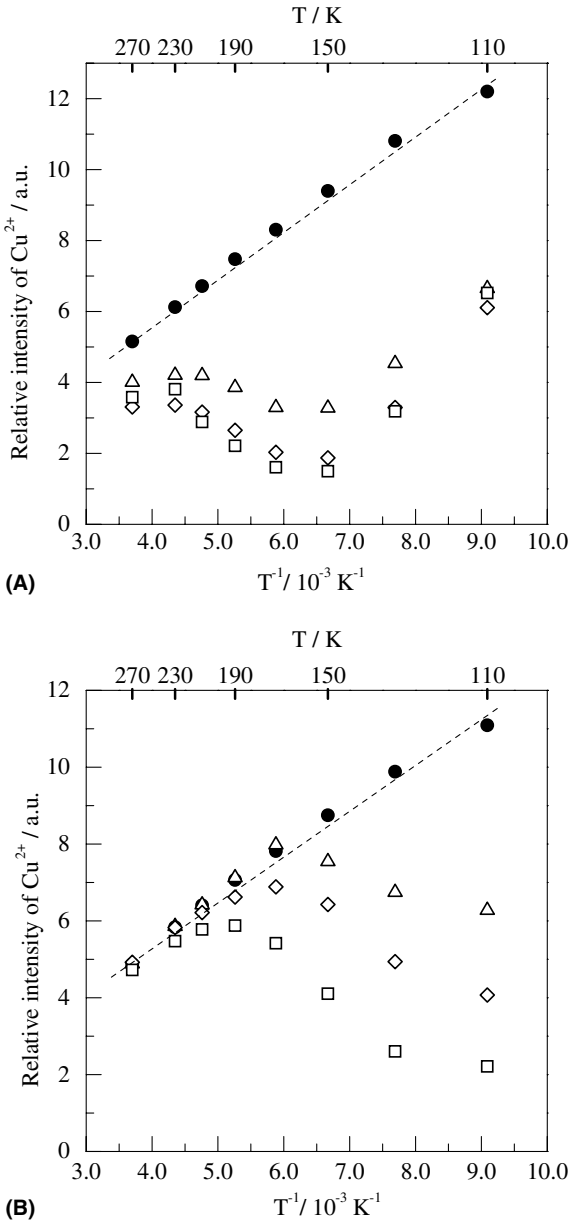


Fig. 2. Change in the relative EPR signal intensities of CuNa-FAU with (A) NO and (B) $O_2$ as a function of measurement temperature. The amounts of $O_2$ and NO introduced were (●) 0, (△) 1.0, (◆) 2.0, and (□) $3.0 \times 10^{-4}$ mol, respectively. The dotted line indicates the Curie's paramagnetic law.

at higher temperatures, 110–270 K. Furthermore, the NO molecule interacting with the $Cu^{2+}$ ion in the zeolite may be classified into the following two types: One is a magnetic electron spin-electron spin dipole interaction between NO and $Cu^{2+}$ both having one unpaired electron (hole). Note that this NO molecule can be EPR silent due to the above reason. The second is a charge transfer type of diamagnetic complex formation such as $Cu^+NO^-$. The present EPR observation suggested that the interaction between NO and $Cu^{2+}$ is thermally reversible. This result may lead us to rule out the latter

possibility ($Cu^{+}NO^{-}$ formation). Thus, the present EPR results are explained in terms of the magnetic interaction of electron spin–spin dipolar coupling as will be seen in the following sections.

The temperature dependence of the EPR spectra of CuNa-FAU was examined in the presence of NO, as shown in Fig. 3. The changes in both spectral feature and intensity were completely reversible in the temperature range from 110 to 270 K. When the EPR spectra of CuNa-FAU with NO (Fig. 3) were compared with those without NO (Fig. 1) at the same temperature, it can be seen that there are clear differences between both spectra, that is, the original signals of the parallel and perpendicular components due to isolated $Cu^{2+}$ (A) and $Cu^{2+}$ (B) almost disappeared because of, probably, line-width broadening for the sample of CuNa-FAU with NO. The signal intensity of CuNa-FAU with NO was also plotted against $T^{-1}$, as shown in Fig. 2(A). In contrast to the case of "pure" CuNa-FAU, no linear relationship was observed between the EPR intensity and $T^{-1}$. These results suggest that the paramagnetic $Cu^{2+}$ ion exchanged into FAU zeolite was magnetically interacted with the introduced NO so as to lead to the line-width broadening of the isolated $Cu^{2+}$ EPR signals.

As can be seen in Fig. 2(A), the signal intensity initially decreased with the increment of temperature (in the range from 110 to 150 K), and simultaneously, the line-width became broader so as to smear the signals due to isolated $Cu^{2+}$ (A) and $Cu^{2+}$ (B) (Fig. 3). The minimum signal intensity was obtained at 150–170 K, regardless of the amount of introduced NO molecules. A further increase in the temperature resulted in the recovery of the signal intensity.

### 3.3. EPR spectra of CuNa-FAU in the presence of $O_2$

Fig. 4 shows the temperature dependency of the EPR spectra for CuNa-FAU in the presence of $O_2$ molecules. The relative EPR signal intensities evaluated from the experimental spectra are plotted against $T^{-1}$ for four samples with different $O_2$ pressures in Fig. 2(B). It can be seen in Fig. 2(B) that the temperature dependency of the signal intensities for CuNa-FAU with $O_2$ is significantly different from "pure" CuNa-FAU without $O_2$ and with NO (see Fig. 2(A)). For example, the signal intensity for CuNa-FAU with $1.0 \times 10^{-4}$ mol $O_2$ increased with increasing temperatures from 110 K. But, after reaching its maximum value at ca. 170 K, the intensity started to decrease following the Curie's paramag-

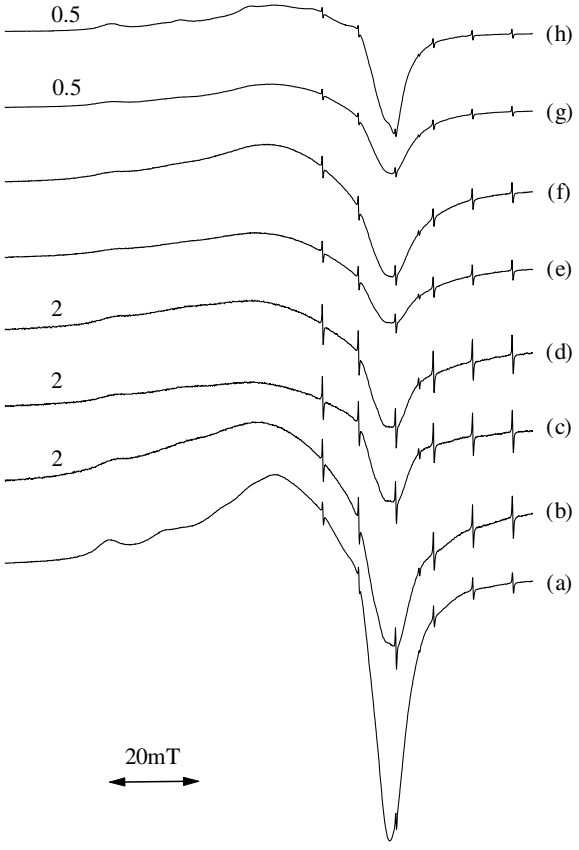


Fig. 3. EPR spectra of CuNa-FAU with NO ($2.0 \times 10^{-4}$ mol), recorded at (a) 110, (b) 130, (c) 150, (d) 170, (e) 190, (f) 210, (g) 230, and (h) 270 K.

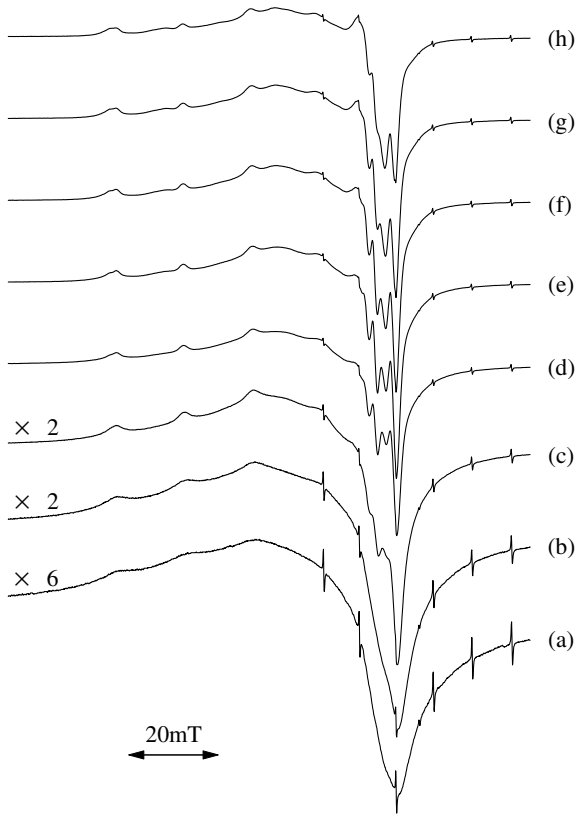


Fig. 4. EPR spectra of CuNa-FAU with $O_2$ ($2.0 \times 10^{-4}$ mol), recorded at (a) 110, (b) 130, (c) 150, (d) 170, (e) 190, (f) 210, (g) 230, and (h) 270 K.

netic law with increasing temperatures. The temperature at which the maximum signal intensity was achieved was dependent on the amount of $O_2$ introduced.

### 3.4. Magnetic interaction between Cu (II) ions and NO or $O_2$ molecules

As mentioned in Sections 3.2 and 3.3, the EPR spectral line shape and intensity of CuNa-FAU were largely influenced by the presence of paramagnetic molecules in the system. It is certain that the observed deviation of the EPR signal intensity from the paramagnetic Curie's law in the low temperature region for the systems, NO + CuNa-FAU and $O_2$ + CuNa-FAU, originates from the line-width broadening. The magnetic interaction between the paramagnetic $Cu^{2+}$ ions and paramagnetic molecular NO or $O_2$ may bring the line-width broadening beyond EPR detectable levels. To support this argument, we measured the magnetic susceptibility of CuNa-FAU with NO and $O_2$, as shown in Fig. 5. The magnetic susceptibility of "pure" CuNa-FAU linearly increased with increasing $T^{-1}$, indicating that the magnetic susceptibility obeys Curie's law. However, no linear correlation could be obtained between the observed magnetic susceptibility of CuNa-FAU with a paramagnetic molecule, NO or $O_2$, and $T^{-1}$. The magnetic susceptibility of CuNa-FAU with NO was higher than that of "pure" CuNa-FAU at 270 K, suggesting that NO molecules start to be adsorbed on CuNa-FAU at this temperature. With further decreasing temperatures, the magnetic susceptibility sharply increased below ca. 230 K, reached a maximum value at ca. 150 K, and then gradually decreased. This temperature dependency is antisymmetrical to that of EPR signal intensity as can be seen in Fig. 2(A), that is, the temperature giving the maximum magnetic susceptibility agreed with the temperature giving the minimum EPR signal intensity. These interesting temperature dependencies in both the magnetic susceptibility and the EPR signal intensity can be interpreted as follows. As mentioned above, it is known that most of the NO molecules are physisorbed on alkaline halides or metal oxides in a diamagnetic NO dimer form, $(NO)_2$, which thermodynamically predominates at lower temperatures [28]. The minimum EPR signal intensity and the maximum magnetic susceptibility for CuNa-FAU with NO may be closely related to the amount of $(NO)_2$ formed on zeolites, that is the formation of diamagnetic $(NO)_2$ may decrease the magnetic susceptibility and at the same time it may decrease the electron spin-electron spin magnetic interaction between the $Cu^{2+}$ ions and NO so as to yield less broad EPR line-widths, as have been observed below 150–170 K. At higher temperatures, the magnetic interaction may become weaker due to the desorption of NO, as a result, and the number of $Cu^{2+}$ ions without NO interaction increases.

The magnetic susceptibility of CuNa-FAU with $O_2$ almost obeys Curie's law above 230 K, but sharply increased below 230 K (Fig. 5). This fact is accounted for by the increase in the amount of paramagnetic $O_2$ molecules adsorbed on the zeolite below 230 K. As seen in Fig. 2(B), the EPR signal intensity obeys Curie's law to 210–230 K and upon further decreasing the the temperature, the intensity decreases monotonously. This, decrement of the EPR signal intensity can be explained by the increase in the electron spin-electron spin magnetic interaction between the $Cu^{2+}$ ions and $O_2$ adsorbed on the zeolite.

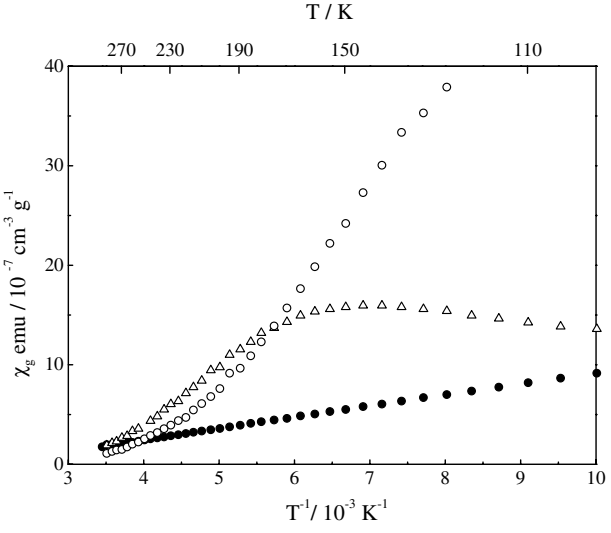


Fig. 5. Magnetic susceptibilities of "pure" CuNa-FAU (●) and CuNa-FAU with $O_2$ (○) or NO (△) molecules.

### 3.5. Application of the Langmuir adsorption model

The EPR signal intensity depended on the amount of NO introduced in the temperature range of 150–210 K where NO molecules are not condensed in the zeolite cavity (see Fig. 2(A)). We considered that the change in the EPR signal intensity was closely related to the adsorption behavior of NO on CuNa-FAU. Assuming that the EPR signal difference ($I_0$–$I_{NO}$) between "pure" CuNa-FAU ($I_0$) and that with NO ($I_{NO}$) corresponds to a degree of the magnetic interaction between paramagnetic $Cu^{2+}$ and NO, the values of $I_0$–$I_{NO}$ are plotted as a function of the amount of NO introduced ($A_{NO}$) to yield quasi-adsorption isotherms at several temperatures. The results are shown in Fig. 6(A). It can be seen in the figure that the $I_0$–$I_{NO}$ value increases with the increment of $A_{NO}$ and it decreases with increasing temperatures.

Now we try to analyse the present experimental results as follows. We assume that (a) the $I_0$–$I_{NO}$ value depends on only the amount of NO adsorbed just on $Cu^{2+}$ and/or on the sites neighboring $Cu^{2+}$; the cupric ions

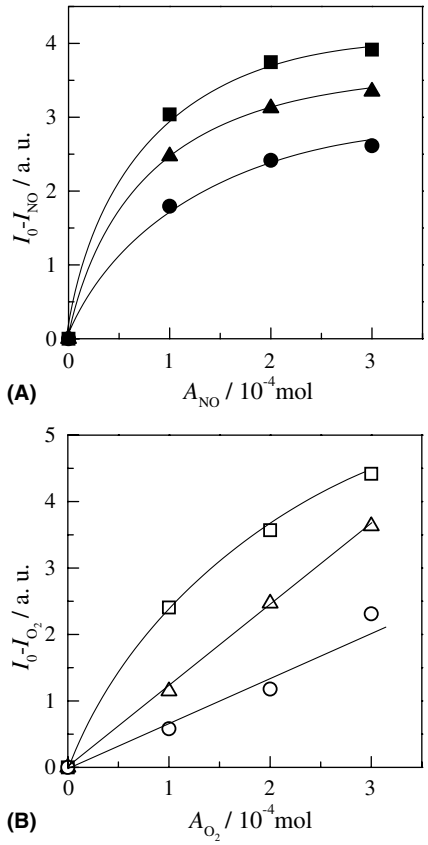


Fig. 6. Plots of (A) $I_0$–$I_{NO}$ EPR signal intensity difference between "pure" CuNa-FAU ($I_0$) and CuNa-FAU with NO ($I_{NO}$), and (B) $I_0$–$I_{O_2}$ against $A_{O_2}$: (●) 190, (▲) 170, (■, ○) 150, (△) 130, and (□) 110 K. Here, $I_0$–$I_{NO}$ (or $I_0$–$I_{O_2}$) stands for the EPR signal difference between "pure" CuNa-FAU ($I_0$) and CuNa-FAU with NO ($I_{NO}$) (or with $O_2$, $I_{O_2}$), and $A_{NO}$ (or $A_{O_2}$) the amount of NO (or $O_2$) introduced.

possibly having a magnetical interaction with the NO molecules and (b) the Langmuir adsorption model for gas–solid interfaces can be applied to the present system. The following equation is given:

$$I_0\text{–}I_{NO} = (Q_L K_L A_{NO})/(1 + K_L A_{NO}), \quad (1)$$

where $Q_L$ and $K_L$ are the Langmuir isotherm constant, representing the monolayer adsorption capacity and equilibrium constant, respectively, and $A_{NO}$ is the amount of NO introduced for a given constant volume, which is replaced by the pressure of NO. The constants, $Q_L$ and $K_L$, can be obtained by linearizing the above equations as follows:

$$A_{NO}/(I_0 I_{NO}) = 1/K_L Q_L + A_{NO} Q_L. \quad (2)$$

The experimental values of $A_{NO}/(I_0\text{–}I_{NO})$ are plotted against the values of $A_{NO}$ in Fig. 7. A good linear relation between the $A_{NO}/(I_0\text{–}I_{NO})$ and $A_{NO}$ values can be obtained with a high correlation coefficient of 0.99 for the data covering three different temperatures of 150, 170, and 190 K. This result suggests that the Langmuir adsorption model can be valid for the present system and the decrease in the EPR intensity of CuNa-FAU

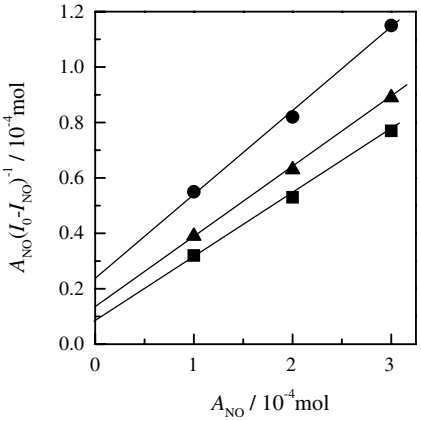


Fig. 7. Plots of $A_{NO}/(I_0\text{–}I_{NO})$ against $A_{NO}$:(●) 190, (▲) 170, and (■) 150 K.

by the introduction of NO above 150 K can be mainly caused by the increase in the amount of NO adsorbed. From the slope ($\equiv 1/Q_L$) and the intercept ($\equiv/(K_{LQL})$) of each line shown in Fig. 7, the constant $K_L$ was evaluated to be 2.50, 1.82, and 1.25 $mol^{-1}$ at 150, 170, and 190 K, respectively. In addition, according to the Clausius–Clapeyron equation, the adsorption enthalpy ($\Delta H_{ad}$) was estimated to be ca. 6.0 kJ $mol^{-1}$. There are no literature data except for the following with reference to the value of $\Delta H_{ad}$; Claudino et al. [29] reported that the $\Delta H_{ad}$ of NO on activated carbon was lower than 10 kJ · $mol^{-1}$.

A similar analysis using the Langmuir adsorption model was carried out for the change in the EPR signal intensity of CuNa-FAU with $O_2$. Fig. 6(B) shows plots of the $(I_0\text{–}I_{O_2})$ values as a function of the amount of $O_2$ introduced ($A_{O_2}$) at three different temperatures of 110, 130, and 150 K; at these temperatures, the deviations in intensity from the Curie's paramagnetic law were observed. The $(I_0\text{–}I_{O_2})$ increased monotonously with an increase in $A_{O_2}$; however, in contrast to the case of CuNa-FAU with NO in the temperature range 150–190 K, no linearity was observed for the plots of $A_{NO}/(I_0\text{–}I_{NO})$ against $A_{NO}$ (not shown here). This result indicates that the isotherm depicted in Fig. 6(B) cannot be represented by the simple Langmuir model in which the monolayer adsorption is postulated, so that the magnetical interaction of copper with $O_2$ may be influenced by not only the amount of adsorbed $O_2$, but also the other factor, for example, the distance between paramagnetic species.

## 4. Conclusion

In the present study, the magnetic interaction between $Cu^{2+}$ ions in CuNa-FAU and adsorbed NO or $O_2$ molecules was investigated by the EPR measurement of $Cu^{2+}$ ions as a function of temperature. In the pres-

ence of NO, the decrease in temperature resulted in a decrease in the EPR signal intensity of $Cu^{2+}$ ions and a minimum EPR intensity was observed at 150–170 K. The signal recovered with a further decrease in temperature. The temperature dependent signal intensities, accompanying the NO adsorption, were discussed in terms of the Langmuir adsorption model in the higher temperature range of 150–190 K and of the diamagnetic $(NO)_2$ dimer formation in the lower temperature range below 150 K.

A similar experiment was carried out for the CuNa-FAU with $O_2$. It was found that $O_2$ molecules behave differently from NO for the adsorption on the CuNa-FAU or magnetic interactions with $Cu^{2+}$ ions in the CuNa-FAU. That is, for the CuNa-FAU system, the EPR signal intensity increased with decreasing temperatures from 270 K, following Curie's law. The maximum EPR intensity was observed at 190–230 K, and then with a further lowering of the temperature, the EPR signal intensity of $Cu^{2+}$ ions decreased with line-width broadening due to magnetic interaction with the $O_2$ molecule adsorbed on the zeolite. The quantitative analysis of the EPR line broadening of CuNa-FAU with $O_2$ will be the subject for a separate paper.

## Acknowledgments

This work was partially supported by a Grant-in-Aid for Science Research from the Ministry of Education, Science, and Culture of Japan (Grant no. 10555312) and the Nippon Sheet Glass Foundation for Materials Science and Engineering.

## References

[1] M.C. Kung, H.H. Kung, Catal. Rev. 27 (1985) 425.
[2] R.A. Schoonheydt, Catal. Rev. 35 (1993) 129.
[3] Y. Kuroda, A. Kotani, H. Maeda, H. Moriwaki, T. Morimato, M. Nagao, J. Chem. Soc., Faraday Trans. 88 (1992) 1583.
[4] D.-J. Liu, H. Robota, Catal. Lett. 21 (1993) 291.
[5] W. Grünert, N.W. Hayes, R.W. Joyner, E.S. Shpiro, M.R.H. Siddiqui, G.N. Baeva, J. Phys. Chem. 98 (1994) 10832.
[6] J. Dedecek, B. Wichterlova, J. Phys. Chem. B 101 (1997) 10233.
[7] K.I. Hadjiivanov, Catal. Rev. 42 (2000) 71.
[8] L. Kevan, in: M. Auerbach, K.A. Carrado, P.K. Dutta (Eds.), Handbook of Zeolite Science and Technology, Marcel Dekker, Inc., New York, 2003, p. 257.
[9] C. Li, Z. Wu, in: M. Auerbach, K.A. Carrado, P.K. Dutta (Eds.), Handbook of Zeolite Science and Technology, Marcel Dekker, Inc., New York, 2003, p. 423.
[10] J.-S. Yu, L. Kevan, J. Phys. Chem. 94 (1990) 7612.
[11] A.M. Prakash, M. Hartmann, L. Kevan, Chem. Mater. 10 (1998) 932.
[12] J. Xu, J.S. Yu, S.J. Lee, B.Y. Kim, L. Kevan, J. Phys. Chem. B 104 (2000) 1307.
[13] S.-K. Park, V. Kurshef, Z. Luan, C.W. Lee, L. Kevan, Micropor. Mesopor. Mater. 38 (2001) 255.
[14] D. Biglino, H. Li, R. Erickson, A. Lund, H. Yahiro, M. Shiotani, Phys. Chem. Chem. Phys. 1 (1999) 2887.
[15] M. Anderson, L. Kevan, J. Phys. Chem. 91 (1987) 4174.
[16] C. Naccache, Y. Ben Taarit, Chem. Phys. Lett. 11 (1971) 11.
[17] Z. Sojka, M. Che, E. Giamello, J. Phys. Chem. B 101 (1997) 4831.
[18] M. Iwamoto, H. Yahiro, K. Tanda, N. Mizuno, Y. Mine, S. Kagawa, J. Phys. Chem. 95 (1991) 3728.
[19] C.C. Chao, J.H. Lunsford, J. Phys. Chem. 57 (1972) 2890.
[20] P.J. Carl, S.C. Larsen, J. Phys. Chem. B 104 (2000) 6568.
[21] K. Pierloot, A. Delabie, M.H. Groothaert, R.A. Schoonheydt, Phys. Chem. Chem. Phys. 3 (2001) 2174.
[22] P.H. Kasai, R.J. Bishop Jr., in: J.A. Rabo (Ed.), Zeolite Chemistry and Catalysis, ACS Monograph 171, Washington, DC, 1976, p. 350
[23] J. Lunsford, J. Phys. Chem. 72 (1986) 4163.
[24] P.H. Kasai, R.J. Bishop Jr., J. Am. Chem. Soc. 94 (1972) 5560.
[25] A. Gutsze, M. Plato, H. Karge, F. Witzel, J. Chem. Soc., Faraday Trans. 92 (1996) 2495.
[26] H. Yahiro, A. Lund, R. Aasa, N.P. Benetis, M. Shiotani, J. Phys. Chem. A 104 (2000) 7950.
[27] H. Yahiro, K. Kurohagi, G. Okada, Y. Itagaki, M. Shiotani, A. Lund, Phys. Chem. Chem. Phys. 4 (2002) 4255.
[28] S. Furukawa, T. Morimoto, R. Hirasawa, J. Phys. Chem. 82 (1978) 1027.
[29] A. Claudino, J.L. Soares, R.F.P.M. Moreira, H.J. José, Carbon 42 (2004) 1483.